

Stable multidomain structures and anomalous Hall effect in the multivalued Sasaki effect in a multivalley semiconductor with inhomogeneities

Z. S. Gribnikov

Semiconductor Institute, Ukrainian Academy of Sciences

(Submitted 20 January 1982)

Zh. Eksp. Teor. Fiz. **85**, 388–399 (July 1983)

Pinning of an interlayer (domain) wall that separates layers with different directions of the Sasaki electric field by the free-electron density inhomogeneities is considered with the Sasaki multivalued effect as the example. It is shown that the walls are located at the density extrema, with a thick wall stable at the minima and a thin one at the maxima. Pinning produces in an inhomogeneous semiconductor a number of variants of stable layered dissipative structures (in contrast to an ideally homogeneous material, where one or two of the simplest structures is stable). In the region of the anomalous Hall effect, an increase of the magnetic field, first, broadens the layers with the Sasaki field directed along the Hall field and narrows the layers with the oppositely directed Sasaki field; second, it leads to a jumplike rearrangement of the layered structure, accompanied by jumps of the transverse emf.

PACS numbers: 75.60.Ch; 75.60.Ej, 72.20.My

INTRODUCTION

The anomalous Hall effect, (AHE), which consists of a steep dependence of the Hall emf on the magnetic field H at small H (Fig. 1), turned out to be most convenient for experimental identification of the multivalued Sasaki effect (MSE) in Refs. 1–3. The AHE was predicted in Ref. 4 from the following considerations. The MSE in an ideally uniform semiconductor causes the latter to be stratified into layers with oppositely directed transverse electric fields (Sasaki fields).^{5,6} At low rates of the surface intervalley relaxation, the stable structure is the simplest two-domain structure with an interlayer boundary in the middle. A weak magnetic field shifts the boundary and broadens the layer with the “correct” sign of the Sasaki field (the sign coinciding with that of the Hall field), and makes the layer with the “incorrect” sign thinner. It is this which causes the AHE: the steep section in Fig. 2 corresponds to displacement of the interlayer wall. Its steepness is a reflection of the fineness of the state with the wall exactly halfway in the sample. When the interlayer wall is moved out to the outer surface of the plate and the Sasaki field becomes of the correct sign in the entire sample, the AHE vanishes; further growth of H causes an increase of the normal Hall emf (gently sloping sections Fig. 1).

Plots of $\mathcal{E}_y = \mathcal{E}_y(H_z)$ similar to the one shown in Fig. 1 were clearly observed experimentally in Refs. 1–3, but their slopes on the AHE section were many times smaller than predicted by the theory.⁴ According to the latter, the slope increases exponentially with increasing ratio d/L_2 , where d is half the thickness of the sample (in the y direction) and L_2 is the length of the electron drift in the electric field (an exact definition is given below) and tends to infinity as $d/L_2 \rightarrow \infty$. Experiment reveals no such tendency. These and a few other deviations from the predictions of the theory^{4–6} were attributed in Ref. 2 to the influence of the sample inhomogeneity.

An attempt is made here to take into account the influence of the inhomogeneities on the layered structure and the AHE in the case of the MSE. A very simple model is used

with a total electron density $2n(y)$, one-dimensionally inhomogeneous along the direction of the Sasaki field (the y -axis direction; the current flows along x and the magnetic field is directed along z). Just as in Refs. 4–6, the calculations are for a two-valley semiconductor. The two-valley-semiconductor model is qualitatively quite satisfactory in the case, e.g., of n -Si at a current along $\langle 110 \rangle$ (see Ref. 2). It will be shown that stable multilayer structures of the Sasaki field E_y are possible in the presence of inhomogeneity. In the absence of density gradient averaged over the thickness ($\langle dn/dy \rangle = 0$) there is likewise no Sasaki field, but in a magnetic field the layered structure becomes rearranged, the fraction of layers with the correct sign of the Sasaki layer increases, that with the incorrect decreases, and it is this which leads to the AHE. The AHE region is limited by the total vanishing of the layers with incorrect sign of the Sasaki field. The slope of the $\mathcal{E}_y = \mathcal{E}_y[H_z]$ plot in Fig. 1 in the region of the AHE is determined by the amplitude of the inhomogeneities. The results indicated are obtained assuming a smooth variation of the inhomogeneities: the characteristic scale is large compared with the drift length L_2 that determines the thickness of the “thick” interlayer walls.

1. BASIC EQUATIONS

We start from the following expressions for the electron fluxes in valleys 1 and 2, located in the xy plane symmetrically about the current direction (the axes) with the large-mass axes at angles $\pm 45^\circ$ to the x axis:

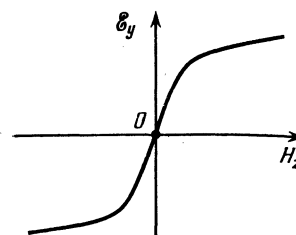


FIG. 1. Hall emf vs the transverse magnetic field in the AHE.

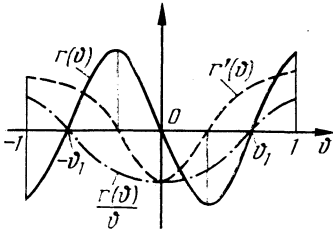


FIG. 2. Qualitative plots of $r(\vartheta)$, $r'(\vartheta)$ and $r(\vartheta)/\vartheta$ in the MSE.

$$j_x^{(1,2)} = -D_{xy}^{(1,2)} \frac{\partial n^{(1,2)}}{\partial y} - (\mu_{xx}^{(1,2)} E_x + \mu_{xy}^{(1,2)} E_y) n^{(1,2)}, \quad (1)$$

$$j_y^{(1,2)} = -D_{yy}^{(1,2)} \frac{\partial n^{(1,2)}}{\partial y} - (\mu_{yx}^{(1,2)} E_x + \mu_{yy}^{(1,2)} E_y) n^{(1,2)}; \quad (2)$$

here $n^{(1,2)}$ are the electron densities in the valleys, $\hat{D}^{(1,2)}$ are their diffusion coefficients, and $\hat{\mu}^{(1,2)}$ are their mobilities. It is assumed that the heating-up change of the diffusion and mobility coefficients is immaterial and can be neglected. For the components of the tensors $\hat{\mu}^{(1,2)}$ we have

$$\mu_{xx}^{(1,2)} = \mu_{yy}^{(1,2)} = \mu, \quad \mu_{yx}^{(1,2)} = \pm a\mu - \alpha\mu, \quad \mu_{xy}^{(1,2)} = \pm a\mu + \alpha\mu, \quad (3)$$

where $0 \leq a \leq 1$, and α is the Hall angle and is proportional to H_z . Similar relations hold also for the D components. Account is taken in (1) and (2) of the homogeneity of the problem along the current direction.

Denoting $n^{(1)} + n^{(2)} = 2n$, $n^{(1)} - n^{(2)} = 2nf$, we have

$$n^{(1,2)} = n(1 \pm f), \quad |f| < 1. \quad (4)$$

In the stationary and quasistationary cases considered below we can assume that there is no transverse current, $j_y^{(1)} + j_y^{(2)} = 0$, so that

$$E_y = -E_x(af - \alpha) - \frac{1}{n} \frac{D}{\mu} \frac{\partial n}{\partial y}; \quad (5)$$

the difference between the transverse electron fluxes can be written in the form

$$j_y^{(1)} - j_y^{(2)} = -2Dn \left[\frac{\partial f}{\partial y} + \gamma(1-f^2) \right], \quad (6)$$

where $\gamma = a\mu E_x/D$; the field E_x is assumed hereafter strictly specified. With allowance for (4), the continuity equation for the difference flux (6) is of the form

$$\frac{\partial}{\partial y} \left[\frac{\partial f}{\partial y} + \gamma(1-f^2) \right] + \left[\frac{\partial f}{\partial y} + \gamma(1-f^2) \right] \frac{1}{n} \frac{dn}{dy} = R(f) + \frac{1}{D} \frac{\partial f}{\partial t}, \quad (7)$$

where

$$R(f) = \frac{1}{D} [(v_1 + v_2)f + (v_1 - v_2)], \quad (8)$$

$v_{1,2}$ are the frequencies (reciprocal times) of the electron transitions from alleys 1, 2 into valleys 2, 1; in the region of existence of the MSE they increase rapidly as the electron gases in the valleys become heated.⁷

We use below the model considered in Ref. 7 for the spatially homogeneous situation, when

$$v_{1,2} = v(E_{1,2}), \quad (9)$$

$E_{1,2}$ are the heating fields in the valleys and given in our case by the equations

$$E_{1,2}^2 = E_x^2 + E_y^2 \pm 2aE_xE_y = E_x^2(1 + \vartheta^2 \pm 2a\vartheta), \quad (10)$$

where $\vartheta = E_y/E_x$. The Hall angle that represents the magnetic field in Eqs. (3) does not enter explicitly in (10).

The essential assumption made in this paper is that relations (9) and (10) are preserved for the spatially inhomogeneous situation. We note that the $\vartheta(y)$ distributions obtained here agree with this assumption, since they are combinations of regions of very gradual variation of ϑ , in which the gradient terms of the fluxes are small, and regions with very drastic variation of ϑ , in which the fluxes $J_y^{(1,2)}$ are conserved, so that the exact form of $R(f)$ does not play a special role. Similar assumptions are frequently made in theories of domain instability.⁸

In view of the adoption of relations (9) and (19), it is convenient to transform in (7) to the variable ϑ ; we then have in place of (7)

$$\begin{aligned} & \frac{\partial^2 \vartheta}{\partial \xi^2} + \frac{2\beta}{a} \left(\vartheta - \alpha + \frac{3}{2} \frac{\alpha_1}{\beta^2} \right) \frac{\partial \vartheta}{\partial \xi} \\ & + \left\{ \frac{1}{\beta^2} \frac{d^2 \alpha_1}{d\xi^2} + \frac{2}{a\beta} \left(\vartheta - \alpha + \frac{3}{2} \frac{\alpha_1}{\beta^2} \right) \frac{d\alpha_1}{d\xi} \right. \\ & \left. - \alpha_1 \left[1 - \frac{1}{a^2} \left(\vartheta - \alpha + \frac{\alpha_1}{\beta^2} \right)^2 \right] \right\} \\ & = r(\vartheta) - \frac{v_1 + v_2}{2\nu(E_x)} \left(\alpha + \frac{\alpha_1}{\beta^2} \right) + \frac{\partial \vartheta}{\partial \tau}, \end{aligned} \quad (11)$$

where

$$\begin{aligned} \xi &= y/L, \quad \tau = 2t\nu(E_x), \quad \beta = \gamma L, \quad L = (D/2\nu(E_x))^{1/2}, \\ \alpha_1 &= \alpha_1(\xi) = \frac{a\beta}{n} \frac{dn}{d\xi}, \quad r(\vartheta) = \frac{1}{2\nu(E_x)} [(v_1 + v_2)\vartheta - a(v_1 - v_2)]. \end{aligned}$$

We are interested next only in the case of a weak magnetic field $|\alpha| \ll 1$ and a smooth inhomogeneity $|\alpha_1| \ll 1$. Equation (11) generates two characteristic spatial scales:

$$\xi_1 \approx 1/\beta = D/a\mu E_x L, \quad \xi_2 \sim \beta = a\mu E_x/2\nu(E_x) L,$$

the first of which, ξ_1 , is much smaller in the considered range of electric fields than the second ξ_2 . (In dimensional units the first scale $L_1 = \xi_1 L$ is the "contracted" diffusion length opposite to the field aE_x , and the second, $L_2 = \xi_2 L$ is the drift length in the field over a time $1/2\nu(E_x)$. The range of fields E_x in which $\xi_2 \gg \xi_1$ is determined by the condition

$$\beta^2 = \gamma^2 L^2 \gg 1. \quad (12)$$

The condition $|\alpha_1| \ll 1$ denotes smallness of the change of $n(\xi)$ over lengths of the order of the second (stretched-out) scale:

$$|\alpha_1| = a \left| \xi_2 \frac{1}{n} \frac{dn}{d\xi} \right| \ll 1. \quad (13)$$

We are interested in magnetic fields for which $|\alpha|$ is of the same order as $|\alpha_1|$. Therefore, taking (12) and (13) into account, we can simplify (11):

$$\begin{aligned} & \frac{\partial^2 \vartheta}{\partial \xi^2} + \frac{2\beta}{a} (\vartheta - \alpha) \frac{\partial \vartheta}{\partial \xi} - \alpha_1(\xi) \left(1 - \frac{\vartheta^2}{a^2} \right) \\ & + \frac{v_1 + v_2}{2\nu(E_x)} \alpha = r(\vartheta) + \frac{\partial \vartheta}{\partial \tau}. \end{aligned} \quad (14)$$

We consider only a range of fields in which the MSE takes the simplest form—the equation $r(\vartheta) = 0$ has three roots: 0, ϑ_1 , and $-\vartheta_1$ (Fig. 2).

2. INFINITE HOMOGENEOUS SAMPLE WITH A SINGLE INHOMOGENEITY

We list first the results obtained for an infinite homogeneous sample without a magnetic field ($\alpha = 0$, $\alpha_1 = 0$). Equation 14 has then the following stationary solutions.

1. Uniform distributions (Fig. 2): $\vartheta = 0$, ϑ_1 , $-\vartheta_1$. A solution with a Sasaki field ($\vartheta = 0$) can be readily verified directly to be unstable, with a characteristic dimensionless fluctuation growth rate

$$-\varepsilon = -r'(0) = -dr/d\vartheta|_{\vartheta=0} > 0$$

(Fig. 2); the solutions ϑ_1 and $-\vartheta_1$, however, are stable with a characteristic fluctuation damping decrement.

$$\varepsilon = r'(\vartheta_1) = dr/d\vartheta|_{\vartheta=\vartheta_1} > 0.$$

2. Distribution with a single interlayer wall. There exist two types of such distributions: a) solutions with a thin wall, to the left of which $\vartheta = -\vartheta_1 < 0$ and to the right $\vartheta = \vartheta_1$ (Fig. 3a); b) solutions with thick wall, to the left of which $\vartheta = \vartheta_1 > 0$ and to the right $\vartheta = -\vartheta_1$ (Fig. 3b). The characteristic size of the thin wall is ξ_1 , and that of the thick one is ξ_2 , i.e., the thick wall is thicker than the thin one by $\sim \beta^2$ times. It is easy to verify that in the spectrum of the intrinsic fluctuation damping decrements of the fluctuations for the distributions with a single wall there is contained a minimal decrement equal to zero. It corresponds to the fluctuations of the shift of the distribution as a whole along the ξ axis: the interlayer wall occupies in space a position of neutral equilibrium. All other fluctuations are rapidly damped.

3. Periodic distributions. In an infinite sample there exist distributions with arbitrary dimensionless spatial periods exceeding

$$\xi_{\min} = 2\pi [-r'(0)]^{-1/2}.$$

Distributions with small amplitude $\vartheta_{\max} \ll \vartheta_1$ have a period close to ξ_{\min} . As ϑ_{\max} approaches ϑ_1 , the period of the spatial oscillations increases, reaching and exceeding $\xi_2 \gg \xi_{\min}$. At periods greatly exceeding ξ_2 , the amplitude ϑ_{\max} is less than ϑ_1 by an exponentially small value. Figure 3c shows spatial oscillations of ϑ with a period considerably larger

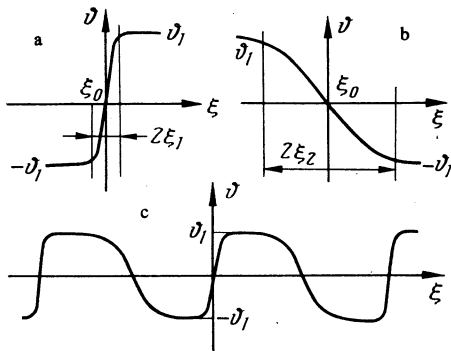


FIG. 3. Distributions $\vartheta(\xi)$ with single interlayer walls and with large spatial period: a) thin wall, b) thick wall, c) distribution with large spatial period.

than ξ_2 . This structure constitutes in practice an alternation of layers with $\vartheta = \vartheta_1$ and $-\vartheta_1$, separated by single thin and thick walls.

The spectrum of the intrinsic decrements for all these distributions contains also a decrement $\varepsilon = 0$ corresponding to a neutral position of the entire structure in space as a whole. It is easy to verify, however, that the zeroth decrement is not a minimum: there exists an infinite number of negative decrements (growth rates), meaning instability of all the periodic structures. They are unstable in a variety of manners. Structures with small amplitude and with a period close to the minimum are just as unstable as the homogeneous unstable solution $\vartheta = 0$. With increasing period, the maximum growth rate decreases, and for structures of the type shown in Fig. 3c it is exponentially small, i.e., such structures should be long-lived.

The solitary inhomogeneity (SI) of the density, introduced here and added to the homogeneous density ($n(\xi) = n_0 + \delta n(\xi)$) satisfies the conditions $\delta n(\pm\infty) = 0$, $d(\delta n)/d\xi = 0$ at $\xi = \pm\infty$ and at one other single point chosen to be the origin ($\xi = 0$). In this case $\alpha_1(\xi)$ has the "dipole" form shown in Fig. 4, where case a corresponds to a single maximum ($\delta n(\xi) > 0$) and case b to a single minimum ($\delta n(\xi) < 0$).

The SI introduced in this manner influences most appreciably the position of a single wall. Taking the position of the wall ξ_0 to mean the coordinate of the point where $\vartheta(\xi_0) = 0$ we obtain in the case of an arbitrarily small inhomogeneity the only possible finite position of the wall: $\xi_0 \approx 0$. Let us demonstrate this.

We seek the distribution $\vartheta(\xi)$ in the presence of a small SI in the form of a sum of a certain distribution $\vartheta_0(\xi)$ in its absence with a small increment $\theta(\xi)$ added:

$$\vartheta(\xi) = \vartheta_0(\xi) + \theta(\xi), \quad (15)$$

where $\vartheta(\xi)$ satisfies Eq. (14) with $\alpha = 0$ and $\partial/\partial\tau = 0$, and $\vartheta_0(\xi)$ satisfies the same equation also with $\alpha_1 = 0$. We have then for $\theta(\xi)$

$$\begin{aligned} \hat{\mathcal{L}}(\theta) &= \frac{d^2\theta}{d\xi^2} + \frac{2\beta}{a} \vartheta_0(\xi) \frac{d\theta}{d\xi} \\ &+ \left[\frac{2\beta}{a} \frac{d\vartheta_0}{d\xi} - r'(\vartheta_0) \right] \theta = \alpha_1(\xi) \left(1 - \frac{\vartheta_0^2(\xi)}{a^2} \right), \\ r'(\vartheta_0) &= \left. \frac{dr(\vartheta)}{d\vartheta} \right|_{\vartheta=\vartheta_0(\xi)}. \end{aligned} \quad (16)$$

We consider first the increment θ in the case when $\vartheta_0(\xi) = \vartheta_1 > 0$ is a homogeneous solution of the problem: $r(\vartheta_1) = 0$. Then a solution of (16), which decreases to zero as $\xi \rightarrow \pm\infty$, takes the form

$$\begin{aligned} \theta &= -\frac{1 - \vartheta_1^2/a^2}{2K(\vartheta_1)} \int_{-\infty}^{\infty} \alpha_1(\xi') d\xi' \exp \left[-\frac{\beta}{a} \vartheta_1 (\xi - \xi') \right. \\ &\quad \left. - |\xi - \xi'| K(\vartheta_1) \right] \\ K(\vartheta_1) &= (r'(\vartheta_1) + \beta^2 \vartheta_1^2/a^2)^{1/2}. \end{aligned} \quad (17)$$

Satisfaction of the condition

$$\beta^2 \gg a^2 r'(\vartheta_1)/\vartheta_1^2, \quad (12')$$

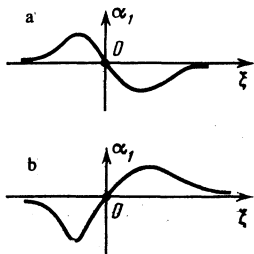


FIG. 4. Two types of SI: a) single maximum b) single minimum.

which is the most accurate concrete modification of (12), enables us to write in place of (17)

$$\theta \cong -\frac{1-\vartheta_1^2/a^2}{2\beta\vartheta_1} a \int_{\xi}^{\infty} \alpha_1(\xi') d\xi' \exp\left[\frac{r'(\vartheta_1)a}{2\beta\vartheta_1} (\xi-\xi')\right]. \quad (18)$$

Finally if

$$\frac{2\beta\vartheta_1}{ar'(\vartheta_1)} \frac{1}{\alpha_1} \left| \frac{d\alpha_1}{d\xi} \right| \ll 1 \quad (13')$$

(a condition close to (13)), we have

$$\theta \cong -\alpha_1(\xi) \frac{1-\vartheta_1^2/a^2}{r'(\vartheta_1)}, \quad (19)$$

i.e., it is a solution of (15) with the derivatives crossed out.

The approximate formula (19) remains fully in force for the increment θ to the solution $\vartheta_0(\xi) = -\vartheta_1$; it is necessary to replace ϑ_1 by $-\vartheta_1$ in the argument of the exponential in the exact Eq. (17), and we obtain in place of (18)

$$\theta \cong -\frac{1-\vartheta_1^2/a^2}{2\beta\vartheta_1} a \int_{-\infty}^{\xi} \alpha_1(\xi') d\xi' \exp\left[\frac{r'(\vartheta_1)a}{2\beta\vartheta_1} (\xi'-\xi)\right]. \quad (20)$$

We proceed now to the solutions $\vartheta_0(\xi)$, which contain the wall. Since the wall position ξ_0 is arbitrary, it is necessary to find that unique value of ξ_0 at which the increment $\theta(\xi)$ turns out to be small. This is simplest to do with the example of a thin wall, whose thickness can be completely neglected if (12') is satisfied, i.e., we regard it as an abrupt step. It follows then from (1) that it is necessary to satisfy on its boundaries the flux-continuity condition

$$j'(\xi) = \frac{d\theta}{d\xi} + \frac{2\beta}{a} \vartheta_0(\xi) \theta; \quad (21)$$

to the left and to the right of the position ξ_0 in (21) it is necessary to substitute for $\vartheta_0(\xi)$ the values $-\vartheta_1$ and ϑ_1 , and for $\theta(\xi)$ respectively the right hand sides of Eqs. (20) and (18). The first term ($d\theta/d\xi$) can be neglected. The equation that determines the unique thin-wall position ξ_0 at which the small inhomogeneity $\alpha_1(\xi)$ disturbs the distribution $\vartheta(\xi)$ little takes the form

$$\int_{-\infty}^{\infty} \alpha_1(\xi) d\xi \exp\left[-\frac{r'(\vartheta_1)a}{2\beta\vartheta_1} |\xi-\xi_0|\right] = 0. \quad (22)$$

At all other wall positions, the inhomogeneity shifts the position itself, i.e., has a strong influence.

When the condition (13') is satisfied, Eq. (22) reduces approximately to

$$\alpha_1(\xi_0) \approx 0, \quad (23)$$

i.e., the narrow wall should be located at $\xi_0 \approx 0$ (Fig. 4). The corrected Eq. (23) takes the form

$$\alpha_1(\xi_0) \approx -\left(\frac{2\beta\vartheta_1}{ar'(\vartheta_1)}\right)^2 \alpha_1''(\xi_0). \quad (23')$$

We proceed now to the situation with the thick wall. The latter is described in the unperturbed system by the equation

$$\frac{2\beta}{a} \vartheta_0 \frac{d\vartheta_0}{d\xi} \cong r(\vartheta_0). \quad (24)$$

For $\theta(\xi)$ we have in the same approximation

$$\frac{2\beta}{a} \vartheta_0(\xi) \frac{d\theta}{d\xi} - \rho(\vartheta_0) \theta \cong \alpha_1(\xi) \left(1 - \frac{\vartheta_0^2(\xi)}{a^2}\right), \quad (25)$$

$$\rho(\vartheta_0) = r'(\vartheta_0) - r(\vartheta_0)/\vartheta_0.$$

The solution of (25) which behaves correctly as $\xi \rightarrow \infty$ and is similar to (18),

$$\theta \cong -\frac{a}{2\beta} \int_{\xi}^{\infty} \alpha_1(\xi') \frac{1-\vartheta_0^2(\xi')/a^2}{\vartheta_0(\xi')} \times \exp\left[-\frac{1}{2\beta} \int_{\xi}^{\xi'} \frac{\rho(\vartheta)}{\vartheta} \Big|_{\vartheta=\vartheta_0(\xi'')} d\xi''\right], \quad (26)$$

behaves just as correctly also as $\xi \rightarrow -\infty$, if

$$\int_{-\infty}^{\xi} \alpha_1(\xi) \frac{1-\vartheta_0^2(\xi)/a^2}{\vartheta_0(\xi)} d\xi \exp\left[-\frac{1}{2\beta} \int_{\xi_0}^{\xi} \frac{\rho(\vartheta)}{\vartheta} \Big|_{\vartheta=\vartheta_0(\xi')} d\xi'\right], \quad (27)$$

The addition replaces (22) in the case of a thick wall. When a condition of the type (13') is satisfied the position of the thick wall is determined by the same equation (23) as for a thin wall, and a $\theta(\xi)$ dependence similar to (19) is obtained directly from (25) if the first term on the left is neglected:

$$\theta(\xi) = -\alpha_1(\xi) \frac{1-\vartheta_0^2(\xi)/a^2}{\rho(\vartheta_0)} \Big|_{\xi_0=0}. \quad (28)$$

To the left and to the right of the inhomogeneity, Eq. (28) goes over into (19), since $r(\pm\vartheta_1) = 0$. The denominator in (28) is positive everywhere except at the point $\xi = 0$ where it, as well as the numerator, is equal to zero.

Thus, a small SI has transformed a problem with infinite degeneracy (relative to the wall position) to a problem with only double degeneracy: the wall can be located only at $\xi_0 \approx 0$, but can be either thin or thick (with alternating solutions $\pm\vartheta_1$ in these cases).

We show now that only one of the two indicated distributions is physically realized, only a thick wall is stable at $\delta n(\xi) < 0$ (a single minimum), only a thin wall is stable at $\delta n(\xi) > 0$ (a single maximum). We consider the evolution of an arbitrary deviation $\delta\vartheta(\xi, 0)$ from the distribution (15). We seek it in the form

$$\delta\vartheta(\xi, \tau) = \delta\theta(\xi) \exp(-\varepsilon\tau),$$

where we obtain for $\delta\theta(\xi)$ the equation

$$\hat{\mathcal{L}}\delta\theta = -\left(\varepsilon + \frac{2}{a^2} \alpha_1(\xi) \vartheta_0(\xi)\right) \delta\theta. \quad (29)$$

Equation (29) with zero right-hand side determines the eigenfunction of the unperturbed problem with zero eigenvalue ε ; this function is

$$\delta\theta_0 = d\theta_0/d\xi \quad (30)$$

and corresponds to the aforementioned neutral position of the wall. The perturbed value of this lowest eigenvalue is

$$\varepsilon = -\frac{2}{a^2} \left\{ \int_{-\infty}^{\infty} d\xi \left(\frac{d\theta_0}{d\xi} \right)^2 \alpha_1(\xi) \theta_0(\xi) \exp \left[2 \frac{\beta}{a} \int_0^{\xi} \theta_0(\xi') d\xi' \right] \right\} \\ \times \left\{ \int_{-\infty}^{\infty} d\xi \left(\frac{d\theta_0}{d\xi} \right)^2 \exp \left[2 \frac{\beta}{a} \int_0^{\xi} \theta_0(\xi') d\xi' \right] \right\}^{-1} \quad (31)$$

At $\xi_0 = 0$ the product $\alpha_1(\xi)\vartheta_0(\xi)$ is of constant sign and positive in the case of a thick wall at a single maximum and of a thin wall at a single minimum (cf. Figs. 3a, b with 4a, b); these are unstable solutions: $\varepsilon < 0$. It is of interest to estimate the real values of the decrements (growth rates) from Eq. (31). In the case of a thin wall we can obtain approximately

$$\theta_0(\xi) \cong \theta_1 \operatorname{th} \frac{\theta_1}{a} \beta \xi, \quad (32)$$

after which the integrals in (31) (at $\alpha_1(\xi) \cong \alpha_1'(0)\xi$) can be calculated exactly:

$$\varepsilon = -\alpha_1'(0)/a\beta. \quad (33)$$

In the case of a thick wall we have with allowance for (24)

$$\varepsilon = -\frac{2}{a^2} \alpha_1'(0) \left\{ \int_{-\theta_1}^{\theta_1} r(\theta) \xi(\theta) d\theta \exp \left[\left(2 \frac{\beta}{a} \right)^2 \int_0^{\theta} \frac{\theta'^2 d\theta'}{r(\theta')} \right] \right\} \\ \times \left\{ \int_{-\theta_1}^{\theta_1} \frac{r(\theta) d\theta}{\theta} \exp \left[\left(2 \frac{\beta}{a} \right)^2 \int_0^{\theta} \frac{\theta'^2 d\theta'}{r(\theta')} \right] \right\}^{-1}, \quad (34)$$

where $\xi(\theta)$ is obtained from the relation $\vartheta = \vartheta_0(\xi)$. An estimate of ε from (34) yields values of the same order as obtained from (33), but of opposite sign.

3. SINGLE INHOMOGENEITY IN A BOUNDED SAMPLE. AGGREGATES OF SINGLE INHOMOGENEITIES

Distinguishing features of a finite-thickness sample are the boundary conditions on the outer lateral surfaces $\xi = \pm \delta$, where $\delta = d/L$. The simplest boundary condition is a complete absence of additional (surface) intervalley relaxation on the surface. Then not only the total transverse current, but also each of its components $j_y^{(1,2)} = 0$ are absent from the surface. When such conditions are imposed on both surfaces of a homogeneous sample, the problem of the distribution of $\vartheta(\xi)$ has a unique solution⁴ characterized by a thin domain wall in the middle ($\xi_0 = 0$, Fig. 5a).

We shall show that a single inhomogeneity of the general position alters this picture radically. We recall that we are considering sufficiently smooth inhomogeneities whose size exceeds the size of the inhomogeneous regions near the surfaces (Fig. 5a). It appears that in those cases when the distribution contains only thin walls, this condition is not necessary.

The procedure of obtaining the distribution is the fol-

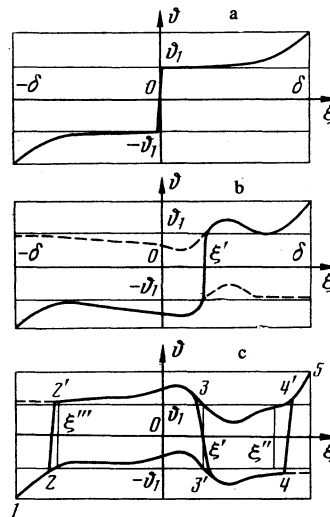


FIG. 5. Distributions of $\vartheta(\xi)$ in a bounded sample in the absence of intervalley relaxation on the surface: a) ideally homogeneous sample, b) sample with single maximum, c) sample with single minimum.

lowing. We obtain two solutions $\vartheta^{(1)}(\xi)$ and $\vartheta^{(2)}(\xi)$ of Eqs. (24) and (25). These solutions satisfy the conditions $\vartheta^{(1)}(\delta) = 1$ and $\vartheta^{(2)}(-\delta) = -1$. We determine next the positions ξ_0 of the thin wall that separates the regions with these solutions. On the thin wall there should be satisfied the flux-continuity condition, which reduces to $\vartheta^{(1)}(\xi_0) = -\vartheta^{(2)}(\xi_0)$.

In the case of a single maximum [Fig. 5b) the solution passes over ϑ_1 everywhere at $\xi > \xi'$ and under it at $\xi < \xi'$; similarly, $\vartheta^{(2)}(\xi) > -\vartheta_1$ at $\xi > \xi'$ and $\vartheta^{(2)}(\xi) < -\vartheta_1$ at $\xi < \xi'$. Therefore the only position of the thin wall is $\xi_0 = \xi'$; the single maximum has drawn the thin wall into itself.

In the case of a single minimum (Fig. 5c) the solution $\vartheta^{(1)}(\xi)$ passes over ϑ_1 everywhere at $\xi < \xi''$, and also on a certain section $\xi > \xi''$ near the sample surface $\xi = \delta$. In the interval $\xi' < \xi < \xi''$ the solution $\vartheta^{(1)}(\xi) < \vartheta_1$. The solution $\vartheta^{(2)}(\xi)$ passes under $-\vartheta_1$ at $\xi > \xi'$, and also at $\xi < \xi'''$ near the surface $\xi = -\delta$; in the interval $\xi''' < \xi < \xi'$ we have $\vartheta^{(2)}(\xi) > -\vartheta_1$. It follows therefore that three positions of the thin wall are possible: $\xi_0 \approx \xi'$, $\xi_0 = \xi_0'' < \xi'''$, $\xi_0 = \xi_0'' > \xi''$ (Fig. 5c). The first of these positions (thin wall in a single minimum) is unstable; the two others can be easily shown to be stable. These two distributions, which contain a thin wall either near the surface $\xi = -\delta$ or near $\xi = \delta$ are by far not all the physically realizable distributions: one more stable distribution is possible, containing both thin walls and a thick wall between them at $\xi \approx \xi'$ (the distribution 1-2-2'-3-3'-4-4'-5 in Fig. 5c).

Another reliable and simple type of boundary condition is infinite rate of intervalley relaxation on the surfaces, when $\vartheta(\pm\delta) = 0$. In this case, in a homogeneous sample, two quasi-single-layer structures are stable⁵: in one case we have almost everywhere $\vartheta(\xi) \cong \vartheta_1$, and in the other $\vartheta(\xi) \cong -\vartheta_1$. A single inhomogeneity, preserving the stability of these structures, adds one more to them. In the case of a single maximum of the density this is a structure with a thin wall at the point $\xi = \xi'$, where $\alpha(\xi') = 0$, and in the case of a single mini-

mum, a structure with a thick wall near $\xi = \xi'$.

Thus, the influence of the SI was reduced to merely a shift of the interlayer wall only in the case shown in Fig. 5b. In all other considered cases the SI increased the number of possible stable distributions.

More vital than the SI are random large-scale distributions of $n(\xi)$, which are characterized by alternation of maxima and minima. We assume that the distance between them exceed as a rule ξ_2 considerably. At each maximum (minimum) of the density there can then be located a thin (thick) interlayer wall, and furthermore any distribution $\vartheta(\xi)$ in which thin and thick walls alternate in succession is stable with respect to small fluctuations. By way of example we consider variants of such alternations in the case of isolated inhomogeneities (clusters) of two types, maximum–minimum and maximum–minimum–maximum. For the first type (Fig. 6a), besides the quasi-homogeneous distributions 1–3–6–1' and 2–4–5–2', there appear two-layer distribution with one interlayer wall, 1–3–4–5–2' and 2–4–5–6–1', as well as distributions 1–3–4–5–6–1' with an internal layer (domain). For the second type (Fig. 6b) are possible two quasi-homogeneous distributions 1–3–6–7–1' and 2–4–5–8–2', three distributions with one wall: 1–3–4–5–8–2', 1–3–6–7–8–2' and 2–4–5–6–7–1', two distributions with two walls 1–3–4–5–6–7–1' and 2–4–5–6–7–8–2', and one distribution with three walls: 1–3–4–5–6–7–8–2'.

It is easy to determine the number P_n of the possible stable distributions in the case of a cluster with n nodes of the function $\alpha_1(\xi)$: $P_n = P_{n-1} + P_{n-2}$. In particular, a ten-wall cluster realizes 144 different stable distributions. The realization of each of these distributions is determined by the prior history (initial conditions and peculiarities of the turning-on process). Neither these questions nor questions of long-time stability of the structures will be considered here.

4. QUALITATIVE PICTURE OF THE AHE

Once a magnetic field is applied ($\alpha \neq 0$) the interlayer walls shift from the positions $\alpha_1(\xi) = 0$, and the character and magnitude of the shift are different for thin and thick walls.

Let us calculate the position of a thin wall. In the pres-

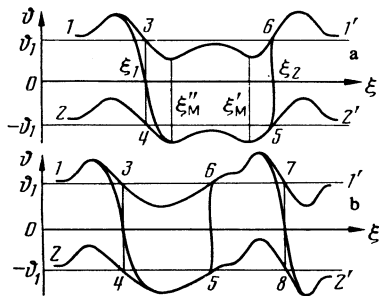


FIG. 6. Distributions $\vartheta(\xi)$ in the case of paired (a) and tripled (b) inhomogeneities.

ence of a magnetic field the increments $\theta(\xi)$ to the homogeneous solutions $\pm \vartheta_1$ are given by (cf. Eq. (19))

$$\theta \approx -\alpha_1(\xi) \frac{1-\vartheta_1^2/a^2}{r'(\vartheta_1)} + \alpha \frac{(v_1+v_2)|_{\vartheta=\vartheta_1}}{2r'(\vartheta_1)v(E_x)}. \quad (35)$$

The continuity conditions for the fluxes on the thin wall, obtained from (21) by replacing here $\theta(\xi_0)$ by $\theta(\xi_0) - \alpha$, lead in place of (23) to the condition

$$\theta(\xi_0) \approx \alpha; \quad (36)$$

from (35) and (36) we obtain for the position of the thin wall

$$\begin{aligned} \alpha_1(\xi_0) &\cong \frac{\alpha}{1-\vartheta_1^2/a^2} \left[\frac{(v_1+v_2)|_{\vartheta=\vartheta_1}}{2v(E_x)} - r'(\vartheta_1) \right] \\ &= -\frac{\alpha\alpha}{1-\vartheta_1^2/a^2} \frac{v_1-v_2}{2v(E_x)} \frac{d}{d\vartheta} \ln \left(\frac{v_1+v_2}{v_1-v_2} \right) \Big|_{\vartheta=\vartheta_1}. \end{aligned} \quad (37)$$

The right-hand side of (37) is positive at $\alpha > 0$, since the ratio $(v_1 + v_2)/(v_1 - v_2)$, which is infinite at $\vartheta \rightarrow 0$, decreases with increasing ϑ and tends to unity. It can be seen from (37) that a thin wall in an infinite sample exists only for sufficiently weak magnetic fields determined by the amplitude $\alpha_1(\xi)$. In a homogeneous sample, however, an arbitrarily weak magnetic field excludes the existence of stable walls.

We proceed now to thick walls. Their existence is due to the equality of the second pair of the separatrices of the saddles $\vartheta^{(1)}(\xi)$ and $\vartheta^{(2)}(\xi)$, which requires that the position of the middle (unstable) quasi-homogeneous root $\theta_0(\xi)$ coincide with α in the presence of inhomogeneity in the magnetic field:

$$\theta_0(\xi) \cong \frac{\alpha - \alpha_1(\xi_0)}{r'(0)} = \alpha \quad (38)$$

or

$$\alpha_1(\xi_0) \cong \alpha(1 - r'(0)). \quad (39)$$

It can be seen from (39) that stable thick interlayer walls, just as thin ones in the presence of a magnetic field, exist in an infinite sample only on account of the inhomogeneities, and a change of the magnetic field shifts their position. With increasing $\alpha > 0$, Eqs. (37) and (39) give the growth of $\alpha_1(\xi_0)$ (we recall that $r'(0) < 0$; see Fig. 2), but the growth rates are given by different expressions and are in general different. Since thick and thin walls exist and are stable at different points of the sample (at the minima and maxima of $n(\xi)$), respectively, it can be easily seen that the magnetic field shifts them in different directions, i.e., counter to each other: at $\alpha > 0$ the thick walls are shifted to the right everywhere on Figs. 5 and 6, and the thin ones to the left. This shift broadens the layers with $\vartheta(\xi) \approx \vartheta_1$, i.e., with the "correct" sign of the Sasaki field, and makes thinner layers with $\vartheta(\xi) \approx -\vartheta_1$, i.e., with the "incorrect" sign. The continuous process of narrowing of the layers with the incorrect Sasaki field continues, however, not until they thin-out completely. With increasing α , one of the interlayer walls moving counter to the other reaches a position in which $\alpha_1(\xi)$ has a local maximum. This occurs, for example, when the thin wall 5–6 in Fig. 6a, after shifting to the left, occupies the position ξ'_m , or else the thick wall 3–4 in the same figure occupies after shifting to the right the position ξ''_m . These

positions of the interlayer walls are the limits. Further increase of α causes either a jump of the wall to a new position with conservation of the previous sequence of alternation of the thin and thick walls (a possibility of which appears on Fig. 6a), or eliminates the wall completely. In the former case one of the layers with the incorrect sign of the field becomes narrower jumpwise, after which a more radical rearrangement of the layered structure takes place, wherein at least one of the layers with the incorrect sign of the field vanishes.

The AHE comprises thus a superposition of two processes: 1) a smooth thinning of the layers with incorrect sign of the field and a thickening of the ones with the correct sign; a jumpwise thinning or vanishing of the layers with incorrect sign of the field. The processes of the second kind should appear when the characteristics of the AHE are carefully and continuously recorded in experiment, and should lead to singularities analogous to the Barkhausen effect in ferromagnets.

CONCLUSION

1. Realization of concrete layered structures from among the multitude of the possible ones is determined, as already noted, by the singularities of the transient process. We point out a circumstance that favors the formation of a distribution with a maximum possible number of layers. Prior to application of the heating electric field E_x there exists in the sample an electric field

$$E_y^0 = -\frac{kT}{e} \frac{1}{n} \frac{dn}{dy},$$

due to the inhomogeneous distribution $n(y)$ and differing

only by a constant negative factor from $\alpha_1(\xi)$. At different points this field is so directed that when a strong heating field E_x is applied to the sample and when transverse fluxes $f_y^{(1,2)}$ connected with E_x appear, the field serves as trigger for a structure with a maximum number of layers, when walls are produced at each zero of the function $\alpha_1(\xi)$. The role of the trigger is played here by the heating (cooling) action of the powers $E_y^0 j_y^{(1,2)}$.

2. Since the experiment^{1,2} is performed under conditions of weak ionization of the donor levels in silicon, the inhomogeneity can be caused not only by the technological inhomogeneity of the sample, but also by the non-uniformity of the temperature. Temperature gradients, by causing density gradients, influence sensitively the layered structure.

The author thanks V. A. Kochelap for a discussion.

¹M. Asche, H. Kostial, and O. G. Sarbey, *J. Phys. C: Sol. St. Phys.* **13**, 645 (1980).

²M. Asche, Z. S. Gribnikov, V. M. Ivashchenko, H. Kostial, V. V. Mitin, and O. G. Sarbey, *Zh. Eksp. Teor. Fiz.* **81**, 1347 (1981) [*Sov. Phys. JETP* **54**, 715 (1981)]. Preprint No. 4, Phys. Inst. Ukr. Acad. Sci., 1981.

³M. Asche, Z. S. Gribnikov, V. M. Ivastchenko, H. Kostial, and V. V. Mitin, *Phys. Stat. Sol. (b)* **114**, 429 (1982).

⁴Z. S. Gribnikov and V. V. Mitin, *Fiz. Tekh. Poluprov.* **9**, 276 (1975) [*Sov. Phys. Semicond.* **9**, 180 (1975)].

⁵Z. S. Gribnikov and V. V. Mitin, *Pis'ma Zh. Eksp. Teor. Fiz.* **14**, 272 (1971) [*JETP Lett.* **14**, 182 (1971)].

⁶Z. S. Gribnikov and V. V. Mitin, *Phys. Stat. Sol. (b)* **63**, 153 (1975).

⁷Z. S. Gribnikov, V. A. Kochelap and V. V. Mitin, *Zh. Eksp. Teor. Fiz.* **59**, 1828 (1970) [*Sov. Phys. JETP* **32**, 991 (1971)].

⁸V. L. Bonch-Bruevich, I. P. Zvyagin, and A. G. Mironov, *Domain Electric Instabilities in Semiconductors*, Consultants Bureau, 1975.

Translated by J. G. Adashko